

RESEARCH ARTICLE

# Development of endocytosis, degradative activity, and antigen processing capacity during GM-CSF driven differentiation of murine bone marrow

Adesola C. Olatunde, Laura P. Abell, Ashley E. Landuyt, Elizabeth Hiltbold Schwartz\*

Department of Biological Sciences, Auburn University, Auburn, Alabama

\* [ehs0009@auburn.edu](mailto:ehs0009@auburn.edu)



**OPEN ACCESS**

**Citation:** Olatunde AC, Abell LP, Landuyt AE, Hiltbold Schwartz E (2018) Development of endocytosis, degradative activity, and antigen processing capacity during GM-CSF driven differentiation of murine bone marrow. *PLoS ONE* 13(5): e0196591. <https://doi.org/10.1371/journal.pone.0196591>

**Editor:** Fabrizio Mattei, Istituto Superiore di Sanità, ITALY

**Received:** October 8, 2017

**Accepted:** April 16, 2018

**Published:** May 10, 2018

**Copyright:** © 2018 Olatunde et al. This is an open access article distributed under the terms of the [Creative Commons Attribution License](https://creativecommons.org/licenses/by/4.0/), which permits unrestricted use, distribution, and reproduction in any medium, provided the original author and source are credited.

**Data Availability Statement:** All relevant data are within the paper and its Supporting Information files.

**Funding:** This work was supported National Institutes of Health, National Institutes of Allergy and Infectious Diseases, Grant R15 AI107773. The funder had no role in study design, data collection and analysis, decision to publish, or preparation of the manuscript.

## Abstract

Dendritic cells (DC) are sentinels of the immune system, alerting and enlisting T cells to clear pathogenic threats. As such, numerous studies have demonstrated their effective uptake and proteolytic activities coupled with antigen processing and presentation functions. Yet, less is known about how these cellular mechanisms change and develop as myeloid cells progress from progenitor cells to more differentiated cell types such as DC. Thus, our study comparatively examined these functions at different stages of myeloid cell development driven by the GM-CSF. To measure these activities at different stages of development, GM-CSF driven bone marrow cells were sorted based on expression of Ly6C, CD115, and CD11c. This strategy enables isolation of cells representing five distinct myeloid cell types: Common Myeloid Progenitor (CMP), Granulocyte/Macrophage Progenitor (GMP), monocytes, monocyte-derived Macrophage/monocyte-derived Dendritic cell Precursors (moMac/moDP), and monocyte-derived DC (moDC). We observed significant differences in the uptake capacity, proteolysis, and antigen processing and presentation functions between these myeloid cell populations. CMP showed minimal uptake capacity with no detectable antigen processing and presenting function. The GMP population showed higher uptake capacity, modest proteolytic activity, and little T cell stimulatory function. In the monocyte population, the uptake capacity reached its peak, yet this cell type had minimal antigen processing and presentation function. Finally, moMac/moDP and moDC had a modestly decreased uptake capacity, high degradative capacity and strong antigen processing and presentation functions. These insights into when antigen processing and presentation function develop in myeloid cells during GM-CSF driven differentiation are crucial to the development of vaccines, allowing targeting of the most qualified cells as an ideal vaccine vehicles.

## Introduction

Dendritic cells (DC) are specialized immune cells that function in antigen uptake, processing and presentation, and induction of the adaptive immune response [1–3]. DC represent remarkable group of cells found in both lymphoid and non-lymphoid tissues under inflamed

**Competing interests:** The authors have declared that no competing interests exist.

and/or steady state conditions. These cells have been classified into different subsets based on phenotypic and functional profiles [4, 5]. Phenotypically, expression of the integrin CD11c and high levels of MHC class II have been used to broadly identify DC. Subsets of DC are further separated based on expression of CD8, CD4, CD11b, and CD45R [6–8]. The functional attributes used in sub-setting DC include migration potential, antigen uptake capability, processing and presentation to the T cells [2, 9, 10]. Steady state DC, whose differentiation is dependent on Fms-like tyrosine kinase 3-ligand (Flt3L), represent conventional lymphoid resident or migratory DC [11–15]. The steady state DC that include both conventional DC (cDC) and plasmacytoid DC (pDC) differentiate from common DC precursor (CDP) and through an intermediate stage known as pre-DCs [16, 17]. Under inflammatory conditions however, monocyte-derived DC (moDC) development and differentiation is driven by Granulocyte-Macrophage Colony-Stimulating Factor (GM-CSF) [18–21].

Historically, it has been difficult to acquire sufficient numbers of DC directly *ex vivo* for functional analysis. DC are typically present in much lower numbers than lymphocytes in lymphoid organs and are of relatively low abundance in peripheral tissues as well [22]. Thus, for decades, GM-CSF has been a favorite cytokine used to generate large numbers of DC from mouse bone marrow *in vitro* [23–25]. Much of what we understand about the endocytic capacity, proteolytic activity, phagosomal maturation, and antigen processing and presenting function of GM-CSF-driven cells has come from studies on differentiated cells, DC and macrophages [26–30]. Thus, we know comparatively little about the developmental stage at which these functions develop. It is therefore important to investigate the development of these functions in order to identify the most qualified cells for therapeutic uses.

Recent studies have demonstrated the previously unrecognized heterogeneity of bone marrow cultured in GM-CSF [31, 32]. While the GM-CSF-driven culture method is known to generate a large population of CD11c<sup>+</sup>MHCII<sup>+</sup> moDC, the relatively high frequency of monocyte-derived macrophages (moMac) in these cultures had not been appreciated [31]. These two cell types were distinguished based on the expression level of CD11c and MHC class II (moMac are MHCII<sup>lo/int</sup>, moDC are MHCII<sup>hi</sup>) [31]. Our recent study confirmed and extended these findings and identified an intermediate precursor cell, the monocyte-derived DC precursor (moDP), which shares many phenotypic characteristics with moMacs, but are distinguished by higher MHCII expression and ability to give rise to moDC [33]. Thus, this cell type is termed moDP.

To elucidate the functional capacity of each distinct myeloid cell population during GM-CSF driven differentiation, we have developed a sorting strategy that enables the isolation of five distinct myeloid cell populations based on the expression of Ly6C, CD115, and CD11c. The phenotypic profile of these developmental stages is as follows: common myeloid progenitor (CMP): Ly6C<sup>-</sup>CD115<sup>-</sup>CD11C<sup>-</sup>, granulocyte-macrophage progenitor (GMP): Ly6C<sup>+</sup>CD115<sup>-</sup>CD11C<sup>-</sup>, Monocytes: Ly6C<sup>+</sup>CD115<sup>+</sup>CD11C<sup>-</sup>, monocyte-derived macrophages/monocyte-derived DC precursors (moMac/moDP): Ly6C<sup>-</sup>CD115<sup>+</sup>CD11C<sup>+</sup>, and monocyte-derived DC (moDC): Ly6C<sup>-</sup>CD115<sup>-</sup>CD11C<sup>+</sup> [33]. Thus, by isolating each of these populations, we set out to clearly define how the cellular uptake mechanisms, phagosomal acidification, and proteolytic activity change during myeloid cell development, and how these functional mechanisms impact the antigen processing and presentation function of these distinct myeloid cell populations along the developmental pathway.

## Materials and methods

### Mice

C57BL/6, OT-1 (C57BL/6-Tg(TcraTcrb)1100Mjb/J) and OT-II (B6.Cg-Tg(TcraTcrb)425Cbn/J) mice were obtained from Jackson Laboratory. T cells derived from OT-I mice recognize

OVA<sub>257-264</sub> peptide presented by MHC class I (H-2 K<sup>b</sup>), while OT-II mice recognize OVA<sub>257-264</sub> peptide presented by MHC class II (I-A<sup>b</sup>). These mice serve as a source of large numbers of antigen-specific T cells for use in measuring presentation of that antigen (ovalbumin). All mice were housed under specific pathogen free conditions. All experiments were approved by the Auburn University Institutional Animal Care and Use Committee and were performed in accordance with the approved guidelines.

### Antibodies and reagents

Primary antibodies specific for murine CD11c (clone N418), CD206 (MMR) (clone C068C2), CD115 (CSF-1R) (clone AFS98), Dectin-1 (CLEC7A) (clone RH1), MHC class I and MHC class II (I-A<sup>b</sup>) (clone AF6-120) were from Biolegend (San Diego, CA). Ly6C (clone HK1.4) was purchased from Ebioscience and CD36 (clone CRF D2712), CD25 (clone PC61), CD4 (clone RM4-5) and CD8 (clone 53.6.7) were purchased from BD-Bioscience (San Jose, CA). DQ™ ovalbumin, OVA-Alexa 647, Dextran Alexa Fluor<sup>®</sup> 488 (mw 10,000) Anionic Fixable, *Staphylococcus aureus* (wood strain without protein A) BioParticles<sup>®</sup>, Alexa Fluor<sup>®</sup> 488 conjugate pHrodo<sup>®</sup> Green *Escherichia coli* BioParticles<sup>®</sup> were purchased from Molecular Probe (Eugene, Oregon). Nigericin sodium salt was purchased from Enzo Life sciences (Farmingdale, New York). Monensin sodium salt was purchased from Amresco (Solo, Ohio).

### Cells and sorting strategies

Myeloid cells were generated from C57BL/6 bone marrow (isolated from 8–24 week-old mice) as previously described [34]. In brief, bone marrow was harvested from mice and the red blood cells were lysed. The cells were cultured in RPMI media supplemented with 10% fetal calf serum (FCS), glutamine (2 mM) and 10 ng/mL granulocyte-macrophage colony-stimulating factor (GM-CSF). The cultured cells were sorted into 5 distinct myeloid cell populations: CMP, GMP, monocyte, moMac/moDP, and moDC using Beckman Coulter Moflo XDP High Speed Cell Sorter at the Auburn University Flow cytometry facility as described previously [33]. Briefly, cultured cells were harvested on either day 3 (to isolate early progenitor cells) or day 5 (to isolate more differentiated cell types) and stained with antibodies to CD115 (CSF-1R), Ly6C and CD11c. CMP, GMP, Monocyte, moMac/moDP, and moDC were isolated based on the phenotypic profile: Ly6C<sup>-</sup>CD115<sup>-</sup>CD11c<sup>-</sup>, Ly6C<sup>+</sup>CD115<sup>-</sup>CD11c<sup>-</sup>, Ly6C<sup>+</sup>CD115<sup>+</sup>CD11c<sup>-</sup>, Ly6C<sup>-</sup>CD115<sup>+</sup>CD11c<sup>low</sup>, and Ly6C<sup>-</sup>CD115<sup>-</sup>CD11c<sup>+</sup>, respectively. The five isolated cell types (from here on referred to as sorted populations) were re-suspended in growth media and were used for all experiments described below, except where indicated otherwise.

In order to differentiate between the moMac/moDP populations, day 5 cells were stained with antibodies to CD11b, CD11c, and MHC class II. Then, the CD11b<sup>+</sup>CD11c<sup>+</sup> cells were isolated into MHCII<sup>lo</sup>, MHCII<sup>int</sup>, and MHCII<sup>hi</sup> cell populations that correspond to moMac, moDP, and moDC.

### Ex vivo cell isolation

Freshly harvested bone marrow from C57BL/6 mice after lysing of the red blood cells were stained with antibodies to CD115, Ly6C and CD11c. These cells were sorted into CMP, GMP, and Monocytes based on the expression of these phenotypic markers and sorting strategies described above.

### Cell surface receptor staining

Bone marrow cells cultured in GM-SCF were harvested and stained with antibodies to CD36 PE, Dectin-1 PE, CD206 PE, CD115, Ly6C and CD11c from day 3 to 7. About  $2 \times 10^5$  cells were stained with each antibody at a final concentration of  $2 \mu\text{g}/\text{mL}$ , and incubated at  $4^\circ\text{C}$  for 30 min. Following the incubation period, cells were washed three times with ice cold FACS Buffer (PBS supplemented with 3% fetal Bovine serum). Unstained cells or cells stained with only one of the antibodies served as control in order to determine the level of auto fluorescence, compensate for fluorescence spillover, and set the gating boundary. The expression of these receptors was measured using flow cytometry.

### Phagocytosis/Macropinocytosis assay

Cells from each sorted cell population ( $2 \times 10^5$  cells/well) were seeded in a 96 well plates. Dextran ( $0.5 \text{ mg}/\text{mL}$ ) or BioParticles (ratio of 2 particles to 1 cell) were added to the wells. The cells were incubated at either  $37^\circ\text{C}$  or  $4^\circ\text{C}$  (as a negative control) for 1 hr and the uptake of these endocytic tracers was measured using flow cytometry. The uptake capacity of each cell population was calculated by subtracting the mean fluorescence intensity (MFI) of samples incubated at  $4^\circ\text{C}$  from the MFI of samples incubated at  $37^\circ\text{C}$  for 1 hr.

### Phagosomal acidification/pH assay

Sorted cell populations were seeded at  $2 \times 10^5$  cells/well in 96 well plate, and were pulsed with  $10 \mu\text{L}$  pHrodo<sup>®</sup> Green *Escherichia coli* BioParticles<sup>®</sup> for 15 min at  $37^\circ\text{C}$ , and washed twice by adding cold growth media, centrifuge at 1200rpm for 5 min and the supernatant was discarded. Cells were then resuspended in growth media and chased for additional 90 min at  $37^\circ\text{C}$ . At the end of the chase period, the cells were washed once with FACS buffer and analyzed using flow cytometry. The uptake of the BioParticles was measured using flow cytometry. To determine the actual pH of the pHrodo-containing phagosomes, pH calibration buffer containing 50 mM HEPES, 30 mM Ammonium Acetate,  $10 \mu\text{M}$  nigericin, and  $10 \mu\text{M}$  monensin was used. The pH of the calibration buffer was adjusted with HCl to create a standard curve of varying pHs, ranging from pH 2.5 to pH 7.5. After the 90 min chased period, cells from each sorted population were washed with FACS wash buffer and incubated with the pH calibration buffer for 15 min at  $37^\circ\text{C}$  and the samples were analyzed using flow cytometry. A pH standard curve was generated for each population by plotting the MFI of the pHrodo against the pH values. The standard curve equations generated from these graphs were used to predict the actual pH of the pHrodo-containing phagosome in each sorted population.

### Proteolysis assay

The proteolytic capacity of each cell population was determined by incubating  $2 \times 10^5$  cells from each sorted population with  $10 \mu\text{g}/\text{mL}$  DQ<sup>™</sup> ovalbumin (DQ-OVA) for 15 min at  $37^\circ\text{C}$ . After the initial incubation, cells were washed twice with cold growth media (as described above) and chased for additional time points. Degradation of DQ-OVA (increasing fluorescence) was measured using flow cytometry. To control for differences in uptake capacity, sorted cell populations were incubated with both DQ-OVA and OVA-Alexa 647 for 1 hr. DQ-OVA fluorescence was then measured specifically in cells containing OVA-Alexa 647.

### In vitro T cell activation assay

$\text{CD}8^+$  T cells were isolated from spleens of OT-I mice (C57BL/6-Tg(TcraTcrb)1100Mjb/J) and  $\text{CD}4^+$  T cells were isolated from spleens of OT-II mice (B6.Cg-Tg(TcraTcrb)425Cbn/J). About



$6 \times 10^7$  cells were labeled with 5  $\mu\text{M}$  CFSE in Hanks' Balanced Salt Solution at room temperature for 8 minutes while shaking gently every 2–3 mins. This was followed by adding 2 mL FCS for at least 1 min to stop the labelling, washed and counted before incubation with sorted populations. For OT-I cell stimulation, sorted cell populations were seeded in a 96 well plates and incubated with 300  $\mu\text{g}/\text{mL}$  of OVA protein or with 10 nM OVA<sub>257-264</sub> Peptide for 2 hrs followed with direct co-culture with CFSE labeled OT-I T cells. For OT-II cell stimulation, sorted cell populations were seeded in 96 well plates and incubated with either OVA protein (100  $\mu\text{g}/\text{mL}$ ) or OVA<sub>323-339</sub> peptide (1  $\mu\text{M}$ ) for 2 hrs followed with direct co-culture with CFSE labeled OT-II T cells. About  $5 \times 10^4$  of sorted cell populations and  $2.5 \times 10^5$  T cells at a ratio of 1:5 was used for this experiment. T cell proliferation and activation was measured by flow cytometry after day 4 or 5 for OT-I and OT-II T cells, respectively.

### Flow cytometry

Where indicated, cells were stained with appropriate fluorophore-conjugated antibody in ice-cold FACS wash buffer (PBS + 3% FCS) on ice for 30 min. This was followed by washing twice with FACS wash buffer, centrifugation at 1200rpm for 5 min. Prior to acquisition, cells were resuspended in FACS wash buffer and filter through 35  $\mu\text{m}$ . Unstained cells or cells stained with only one fluorophore were used to set the gates. In experiments where cells were loaded with fluorescence tracers, untreated samples serve as control and the gates were set on these untreated samples to determine the baseline fluorescence, and to set the compensation in that channel. Also, the forward and side scatter plots were used to exclude debris and doublets. All data were collected on an ACCURI C6 Flow cytometer (BD Biosciences) and analyzed with FlowJo software (Tree Star).

### Statistical analysis

The statistical analysis was performed using either GraphPad Prism 6 or Statistical Analysis System (SAS) software. All graphs were plotted in GraphPad Prism 6. The effect of treatment between different cell populations was analyzed using one-way analysis of variance (ANOVA), the Tukey multiple comparison PROC GLM procedure. Where indicated, treatments were considered significantly different at  $p < 0.05$ .

## Results

### Expression of uptake receptors during GM-CSF driven differentiation

Myeloid cells are known to express a wide range of uptake receptors such as scavenger receptors [35, 36], mannose receptors, and Dectin-1 [37, 38]. These receptors play important roles in cell adhesion as well as optimizing uptake of different types of particles or antigens. However, the relative expression of these receptors at distinct stages of GM-CSF-driven cell development is not well defined. Thus, we measured the expression of these receptors during GM-CSF driven differentiation of murine bone marrow from days 3 through 7. The heterogeneous populations of bone marrow were stained with antibodies to scavenger receptor (CD36), mannose receptor (MMR, CD206) and Dectin-1 and expression was measured by flow cytometry. There was an increase in the expression of CD36 and CD206 from days three to seven of culture with the expression of these two receptors peaking on day seven (Fig 1A). The expression of Dectin-1 increased from day 3 to day 5, with a slightly decreased expression on day 6 and 7 (Fig 1A). This result suggested that CD36 and CD206 are expressed at later stages during myeloid cell development while Dectin-1 is most highly expressed earlier during development.

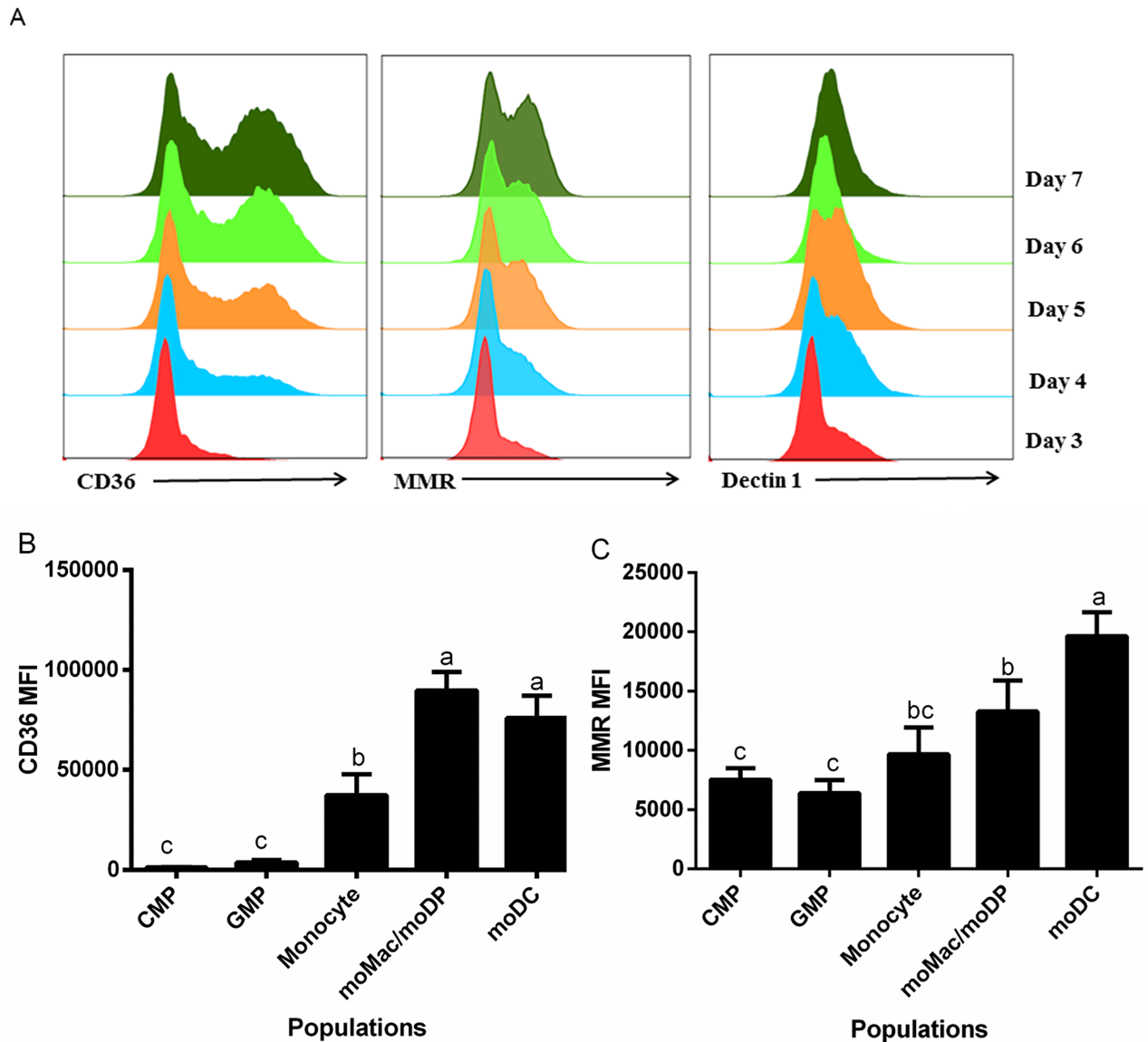


**Fig 1. Differential expression of uptake receptors during GM-CSF driven differentiation.** Bone marrow was harvested from C57BL/6 mice and was cultured in GM-CSF and stained with antibodies to CD36, CD206, or Dectin-1. (A) Representative histograms showing the expression of CD36, CD206, and Dectin-1 from day 3 to 7. Data were compiled from at least three independent experiments showing mean fluorescence intensity (MFI) of (B) CD36 and (C) MMR expression in the five cell populations. Statistical analysis was conducted using one way ANOVA Tukey multiple comparison test. Letters over bars indicate statistically significant differences in means ( $p < 0.05$ ).

<https://doi.org/10.1371/journal.pone.0196591.g001>

We then measured the expression of these receptors with respect to distinct developmental stages, based on Ly6C, CD115 and CD11c expression. Interestingly, moMac/moDP and moDC, which were the dominant cell types on day 6 and 7, had the highest expression of CD36; whereas, CMP and GMP, the most prevalent cell types on day 3, had low expression of CD36 (Fig 1B). These results are consistent with a previous study that found high expression of scavenger receptor in DC, and the expression of this receptor is up-regulated upon DC maturation [39]. In contrast, all of the cell types expressed CD206 at relatively the same level with the exception of moDC that had a slightly increased expression (Fig 1C). This result is consistent with another study that found high expression of CD206 in immature DC [40].

## Distinct uptake capacities exhibited during GM-CSF driven differentiation

Immature DCs are known to utilize both macropinocytosis and phagocytosis as mechanisms of uptake [40–43]. However, endocytic capacity is down-regulated as dendritic cells undergo maturation [41]. What remains to be determined is how uptake capacity changes during development. Thus, to determine the uptake capacity of each myeloid cell population along the developmental spectrum, the sorted cells were fed one of two different endocytic tracers: Alexa-488 dextran (mw 10,000) as a measure of fluid-phase uptake or pinocytosis or Alexa-488 tagged BioParticles (*Staphylococcus aureus* wood strain without protein A), as a measure of phagocytosis. As illustrated by representative histograms (Fig 2A), CMPs demonstrated a low level of dextran uptake above the ice control, at a low level. Pinocytic activity increased only moderately in the GMP population, yet reached its peak in monocytes and moMac/moDP (Fig 2A and 2B). Pinocytic activity of moDC was slightly reduced compared to monocytes and moMac/moDP (Fig 2A and 2B).

The uptake of the larger cargo, BioParticles, followed a similar general trend as dextran uptake with some notable differences. CMP demonstrated virtually no phagocytic capacity (Fig 2A and 2C). Strikingly, GMP exhibited strong phagocytic activity, similar to that of monocytes (Fig 2A and 2C), and considerably stronger than their pinocytic activity (Fig 2B and 2C). Again, monocytes demonstrated the highest uptake capacity, with the highest phagocytic activity (Fig 2C). In contrast to dextran uptake, phagocytic activity also tended to decrease more significantly in moMac/moDP and moDC as demonstrated by decreased BioParticle uptake in these cell types (Fig 2C). These observed differences in uptake capacities of each myeloid cell type reflect significant functional diversity among these cell types.

## Phagosomal acidification increases progressively during GM-CSF-driven development

Acidification of the phagosome is one of the key events of phagosome maturation, and it is important for both antimicrobial and antigen processing functions [44, 45]. To assess the phagosomal pH of each myeloid cell population, we used a pulse-chase approach with pH-sensitive fluorescent particles (pHrodo Green *E. coli* BioParticles, Molecular Probes/Invitrogen). Cells were loaded with the pHrodo particles for 15 min, washed, and chased for additional 90 mins. This allowed us to track the acidification of a synchronized cohort of particles taken up during the short pulse period. Representative histograms of each cell population following the pulse of pHrodo *E. coli* BioParticles are presented in Fig 3A (top panels). Each population had a low background fluorescence indicating minimal acidification at this early time point (Fig 3A and 3B). After the 90 min chase period, phagosomal acidification became evident to different degrees in the five populations. Fluorescence was especially high in the monocyte and moMac/moDP populations (Fig 3A (bottom) and Fig 3B). CMP demonstrated the little to no phagosomal acidification (Fig 3A and 3B). The percent of pHrodo *E. coli* BioParticle-positive cells as well as the MFI of pHrodo gradually increased in GMP and monocytes and peaked in moMac/moDP population, decreasing substantially in moDC (Fig 3B).

Our previous studies indicated that the *Listeria monocytogenes*-containing-phagosomes in DC had a slightly elevated pH compared the same compartment in bone marrow derived macrophages [34]. To better understand phagosomal acidification across the developmental spectrum, we quantitatively compared the phagosomal pH of the five developmental stages driven by GM-CSF. To determine how fluorescence corresponded to actual pH values, standard curves were generated for each cell type in pH-normalized buffers using nigericin and monensin to equilibrate intracellular and extracellular pH. Phagosomal pH decreased progressively from the CMP stage (which was close to neutral pH 7.01) through the moMac/moDP stage which had

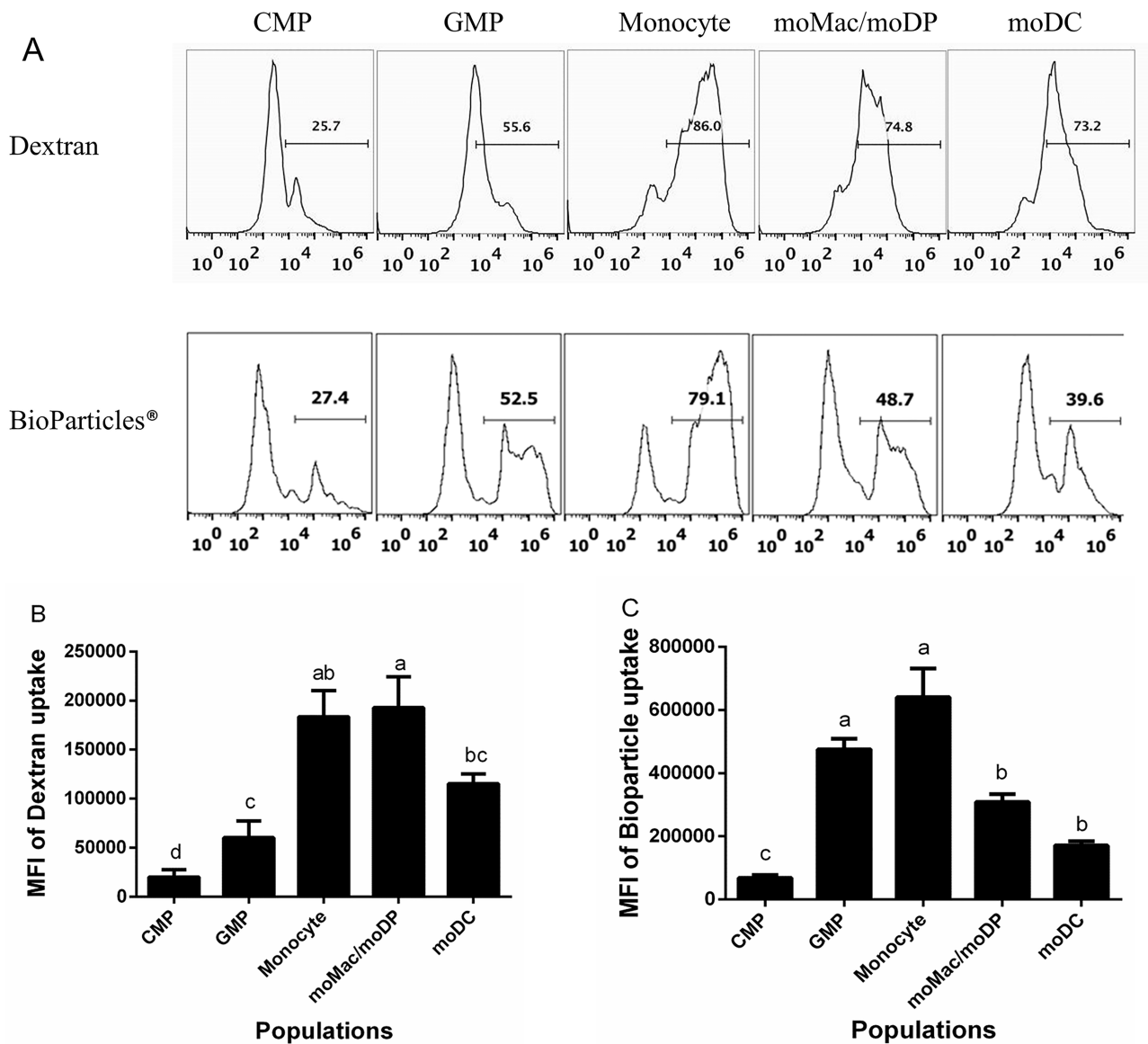


**Fig 2. The uptake capacity of GM-CSF driven myeloid cells increased as cell progress in development and modestly decreased in more differentiated cell types.** Sorted cell populations were fed 0.5 mg/mL Dextran Alexa Flour 488 (10,000 MW) or *S. aureus* BioParticle Alexa flour 594 conjugate for 1 h at 37°C (red), or at 4°C (blue) as negative control. The uptake of the fluorescent tracers was measured by flow cytometry. (A) Representative histograms of Dextran uptake (top panels) and BioParticle uptake (bottom panels) by the five isolated myeloid cell populations. Uptake of dextran (B) and bioparticles (C). Uptake values were calculated by subtracting the MFI of the ice control for each population from the MFI of that population incubated at 37°C. These data are compiled from at least four independent experiments. Statistical analysis was performed using SAS, one-way ANOVA Tukey's multiple comparison tests. Letters over bars indicate statistically significant differences in means ( $p < 0.05$ ).

<https://doi.org/10.1371/journal.pone.0196591.g002>

the lowest pH at ~ pH 4.26. The pH of the moDC population was higher, ~ pH 5.89, which was very similar to monocytes (~5.87). GMP had an average pH of 6.52 (Fig 3C). Thus, these findings support our previous result indicating that moDC have a higher pH than moMac [34, 46]

### Proteolysis is a function exhibited later in the GM-CSF-driven developmental pathway

To elucidate the proteolytic capacity of myeloid cells along the developmental spectrum, we utilized a fluorescence-quenched probe- DQ™ ovalbumin (DQ-OVA) that emits bright green

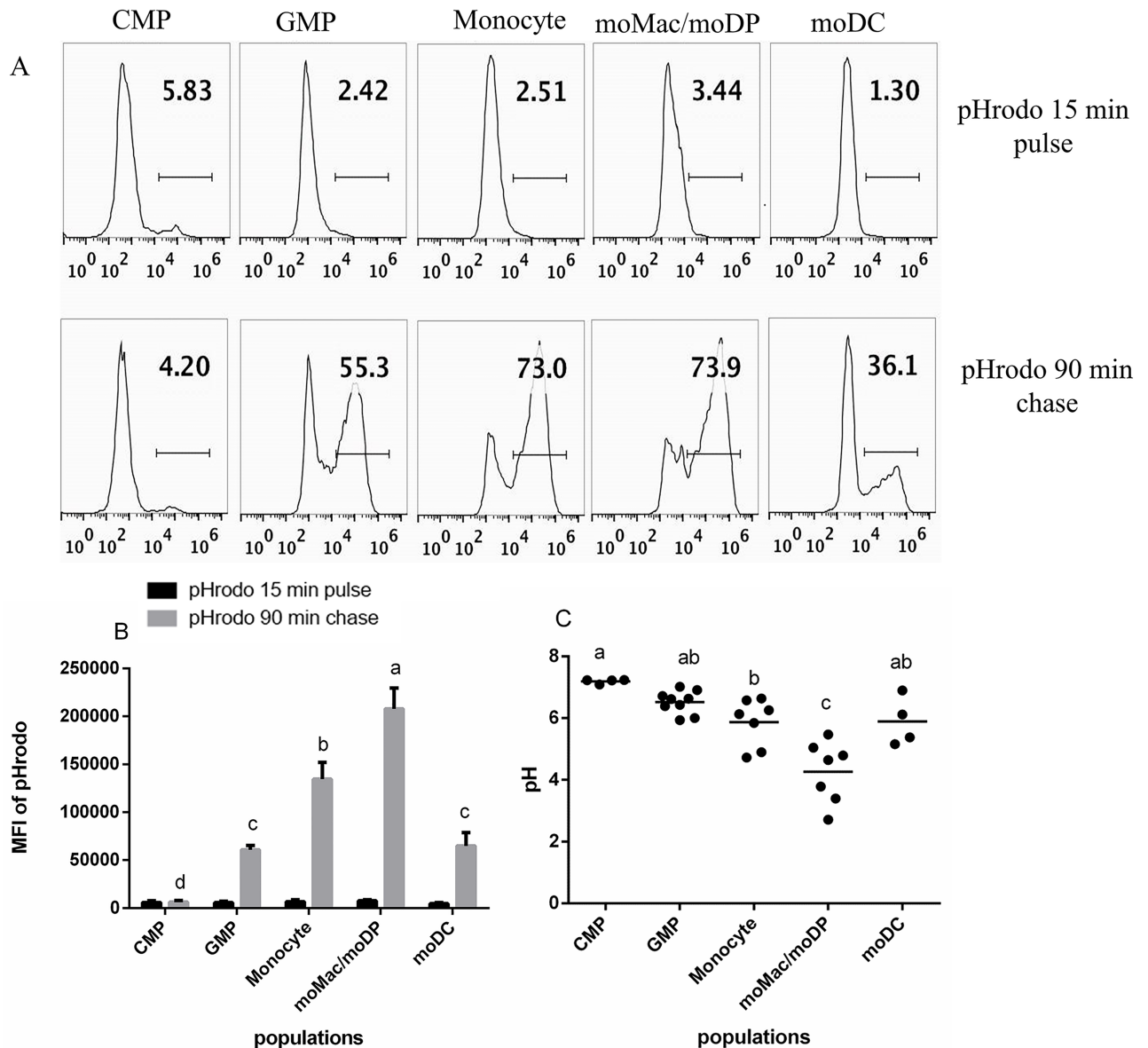


**Fig 3. Phagosomal pH of each developmental stage.** Sorted populations were pulsed with 10  $\mu$ L pHrodo *E. coli* BioParticles for 15 min, washed and chased for 90 min. The uptake of the pHrodo *E. coli* BioParticles and the phagosomal acidification was measured by flow cytometry. (A) A representative histograms of pHrodo *E. coli* BioParticle uptake at 15 min (top) and phagosomal acidification at 90 min (bottom) in all the five isolated populations. (B) The MFI of pHrodo *E. coli* BioParticle uptake at 15 min and 90 min, in all the five isolated myeloid cell populations. Data are compiled from at least four independent experiments. (C) The phagosomal pH of each myeloid cell population was calculated vs a standard curve at varying pHs maintained in Hesper buffer containing nigericin and monensin. The statistical analysis was performed using SAS, one way ANOVA Tukey's multiple comparison test. Letters over bars indicate statistically significant differences in means ( $p < 0.05$ ).

<https://doi.org/10.1371/journal.pone.0196591.g003>

fluorescence upon proteolysis. Each isolated cell population was pulsed with 10  $\mu$ g/mL DQ-OVA for 15 min, washed and chased for additional 30 min, 1 hr, or 2 hr. As expected, there were no significant differences in the fluorescence of DQ-OVA across the populations after the initial 15 min pulse (Fig 4A and 4B) as this was likely too soon to observe degradation. After the 30 min chase, the moMac/moDP and moDC populations showed significant degradative activity evidence by increased fluorescence. This fluorescence was maintained at 1 hr chase, but decreased moderately by 2h, suggesting more complete degradation. In contrast,

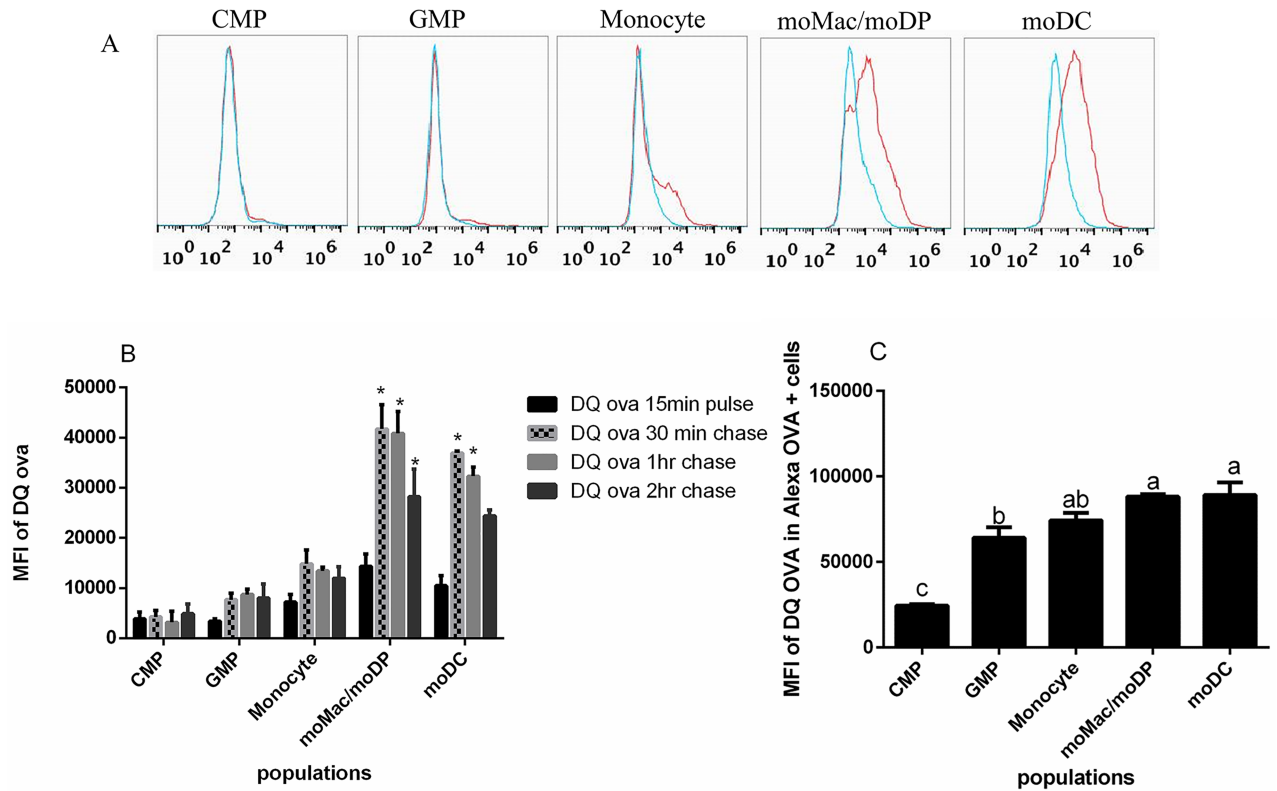


**Fig 4. Proteolytic activity increases as myeloid cells become more differentiated.** Sorted populations were pulsed with 10  $\mu\text{g}/\text{mL}$  DQ™ ovalbumin (DQ-OVA) for 15 min, washed and chased for 30 min, 1hr or 2hr. Proteolysis (indicated by increased fluorescence) of DQ-OVA over time was measured by flow cytometry. (A) A representative histogram of DQ-OVA uptake at 15 min (blue) and degradation at 30 min (red). (B) The MFI of DQ-OVA at 15 min and degradation at 30 min, 1hr and 2hr in all the five isolated myeloid cell populations. (C) The MFI of DQ-OVA degradation only within OVA-Alexa positive cells measured at 1 hr post incubation. Compiled data come from a minimum of three independent experiments. Statistical analysis was conducted using one way ANOVA Tukey multiple comparison test. Asterisk indicate a  $p < 0.05$  when compared with the 15 min pulse.

<https://doi.org/10.1371/journal.pone.0196591.g004>

there was no significant increase in the proteolysis of DQ-OVA by the CMP and GMP populations (Fig 4A and 4B).

To control for any effect that the different uptake capacities of the five populations might have on the degradative measurements (Fig 2), we utilized an additional pH-insensitive tracer, OVA-Alexa 647, in combination with DQ-OVA to track the degradation only within the cells that had taken up the OVA-Alexa 647. In support of the previous result, we found that moMac/moDP and moDC had the highest degradative potential while GMP and Monocytes were slightly less degradative, and there was little to no proteolysis detected in CMP (Fig 4C). The data thus suggest that proteolytic activity is acquired after the CMP stage of myeloid cell development and peaks in the moMac/moDP and moDC stages.

### Antigen processing and presentation function is evident prior to myeloid cells differentiating into moDC

In order to assess the ability of each cell population to process and present antigen, we incubated them with OVA protein or peptide and analyzed their ability to stimulate proliferation and activation of naïve OVA-specific T cells (isolated from OT-I (C57BL/6-Tg(Tcr $\alpha$ Tcr $\beta$ )1100Mjb/J) or OT-II (B6.Cg-Tg(Tcr $\alpha$ Tcr $\beta$ )425Cbn/J) mice). To measure proliferation, T cells



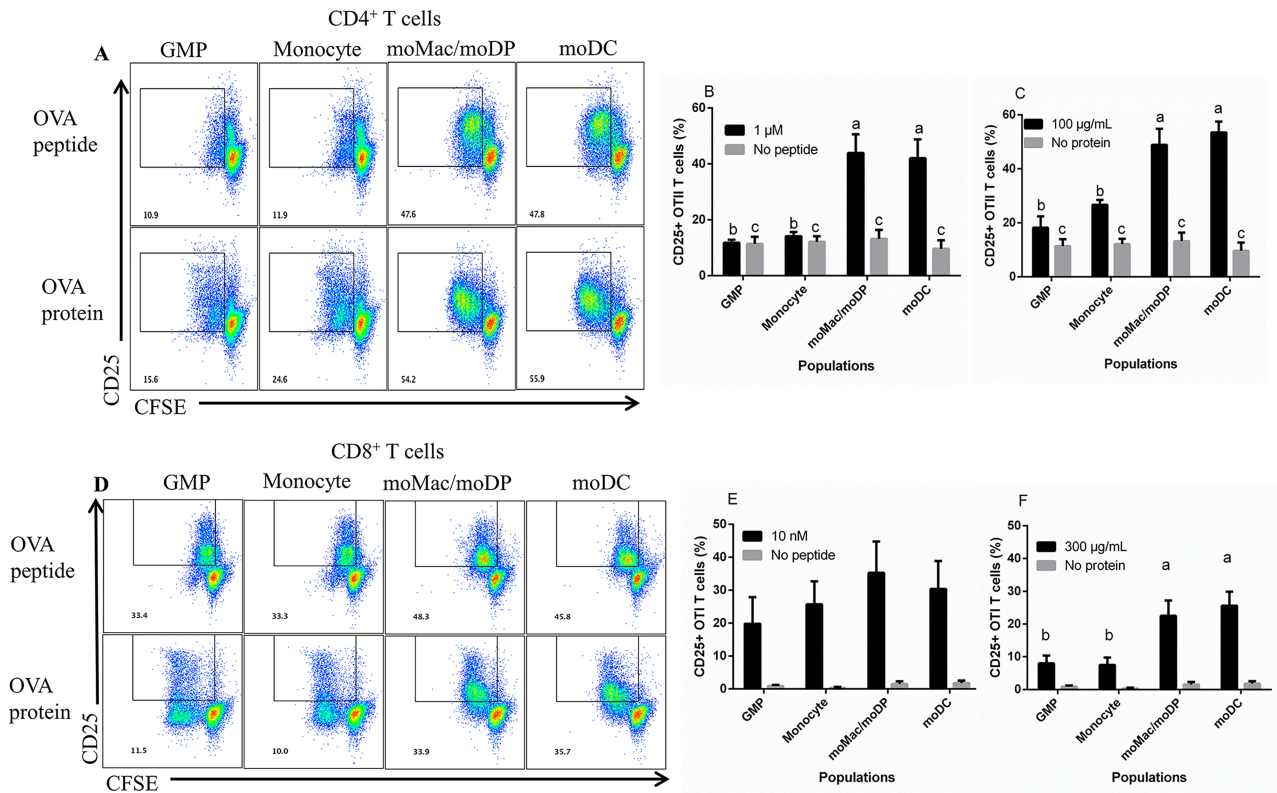


**Fig 5. moMac/moDP and moDC exhibited both antigen processing and presentation functions.** The sorted cell populations were incubated with different concentrations of OVA peptide or OVA protein and co-cultured with CFSE labeled T cells. (A) The dot plots illustrate CD4<sup>+</sup> OT-II T cells stimulated with 1  $\mu$ M of OVA<sub>323-339</sub> (top) or 100  $\mu$ g/mL of OVA protein (bottom). T cell proliferation and activation was measured using CFSE fluorescence dilution at day 5 by flow cytometry. (B) and (C) Compiled data of CD25 expression by OT-II T cells in the presence of OVA peptide (1  $\mu$ M) or OVA protein (100  $\mu$ g/mL), respectively. (D) The dot plots of CD8<sup>+</sup> OT-I T cells stimulated with 10 nM of OVA<sub>257-264</sub> (top) or 300  $\mu$ g/mL of OVA protein (bottom). T cell proliferation and activation was measured at day 4 by flow cytometry. (E) and (F) CD25 expression by OT-I T cells in the presence of OVA peptide (10 nM) or OVA protein (300  $\mu$ g/mL), respectively. Compiled data are derived from a minimum of 3 independent experiments. Statistical analysis was conducted using one-way ANOVA Tukey multiple comparison test. Letters over bars indicate statistically significant differences in means ( $p < 0.05$ ).

<https://doi.org/10.1371/journal.pone.0196591.g005>

were stained with CFSE prior to culture with each population and activation was measured based on CD25 expression.

To assess antigen-presenting capacity, OVA peptides were used as the antigen source. GMP and monocyte populations were unable to stimulate robust OT-II proliferation and CD25 up-regulation when loaded with OVA<sub>323-339</sub> compared to the no antigen control (Fig 5A and 5B; S2A, S2B and S2C Fig). However, GMP and monocytes were able to stimulate significant proliferation of OT-I T cells when loaded with OVA<sub>257-264</sub> (Fig 5D and 5E; S2D, S2E and S2F Fig). As a point of comparison, GMP and monocytes also had the lowest expression of MHC class II molecules, yet were similar in MHC class I expression (S1 Fig). Thus, the poor stimulatory capacity of GMP and monocytes to activate CD4<sup>+</sup> T cells might be attributed to their lower expression of MHC class II molecules as well as reduced proteolytic activity (Fig 5B). In contrast, moMac/moDP and moDC were able to stimulate strong proliferation and activation of both OT-II and OT-I T cells when loaded with peptide (Fig 5A, 5B, 5D and 5E; S2A, S2B and S2C Fig).

Antigen processing capacity was tested using soluble OVA protein as the antigen source. GMP and monocytes were able to induce minimal activation and proliferation of OT-II cells

when loaded with OVA protein (Fig 5A and 5C). Again, moMac/moDP and moDC induced the strongest OT-II proliferation and activation when loaded with OVA protein, indicating their strong antigen processing and presentation capacities (Fig 5D and 5F). Interestingly, when we assessed their cross presentation potential using OVA protein to stimulate OT-1 T cell activation, we observed that both moMac/moDP and moDC were potent at cross-presenting the protein antigen, while GMP and monocytes induced OVA-specific CD8<sup>+</sup> T cell proliferation but induced lower level up regulation of CD25 (Fig 5D and 5F).

CMP induced little CD4<sup>+</sup> or CD8<sup>+</sup> T cell proliferation or CD25 expression in the presence of OVA protein or OVA peptide (data not shown). This observation was not surprising given that CMP had minimal uptake capacity, proteolytic activity and phagosomal acidification.

### The moMac and moDP population have similar functional capacities

We had previously determined that moMac/moDP and moDC (all CD11c<sup>+</sup>) could further be sub-divided based on the expression of CD11b and MHC class II (MHCII), with MHCII<sup>lo</sup>, MHCII<sup>int</sup>, and MHCII<sup>hi</sup> cell types corresponding to moMac, moDP and moDC, respectively [33]. In order to examine the functional differences between the moMac, moDP and moDC populations, cells were isolated into three populations based on the expression of these molecules as previously described [33]. We observed that MHCII<sup>lo</sup> population had the highest phagocytic capability, with a slightly lower BioParticle uptake by MHCII<sup>int</sup>, and the MHCII<sup>hi</sup> cells had the least phagocytic activity (Fig 6A and 6B). The observed decrease in the uptake potential of MHCII<sup>hi</sup> population especially when compared to the MHCII<sup>int</sup> precursor cell, moDP, supports the concept that as DC become more differentiated toward maturation, they down-regulate their endocytic capacity [41].

In addition, we measured the phagosomal pH in each population and found that MHCII<sup>lo</sup> and MHCII<sup>int</sup> had highly increased fluorescence at 90 min at a level higher than the background fluorescence observed at 15 min after the initial incubation with pHrodo (Fig 6C and 6D). Interestingly, we found that MHCII<sup>lo</sup> and MHCII<sup>int</sup> had an average pH 4.76 and 3.82, respectively (Fig 6E), a pH comparable to that observed in moMac/moDP (pH 4.26) (Fig 3). However, MHCII<sup>hi</sup> populations still demonstrated the highest phagosomal pH, with an average pH 5.68 (Fig 6E), a pH closer to that observed in moDC (Fig 3).

Finally, we assessed the proteolytic activity of these cells by utilizing DQ-OVA. There was a slight increase in the fluorescence of the DQ-OVA across all populations between the initial 15 min pulse and the 30 min chase (Fig 6F and 6G), with MHCII<sup>int</sup> demonstrating the highest proteolysis at the 30 min chase period. However, when we utilized the OVA-Alexa 647 to control for differential levels of uptake, (examining only the cells that had taken up the OVA-Alexa 647), we observed that both MHCII<sup>int</sup> and MHCII<sup>hi</sup> had a slightly higher degradation potential when compared to the MHCII<sup>lo</sup> population (Fig 6H). Taken together, these results indicate that the moMac population had the highest phagocytic activity, moderate pH and mild proteolysis while the moDP population was slightly less phagocytic and had the lowest phagosomal pH and highest degradative activity. Finally, the moDC population had greatly reduced phagocytosis, more neutral pH and moderate degradative activity.

### Functional capacity of early progenitors isolated directly ex vivo

Finally, to ensure that our functional analyses were reflective of those observed *in vivo*, we examined the functional capacity of early progenitor cell types CMP, GMP, and monocytes freshly isolated from bone marrow. We found that CMP had the lowest uptake capacity, followed with increased uptake of Bioparticles in GMP, and the monocyte population had the highest uptake capacity (Fig 7A and 7B). Consistent with our *in vitro* studies (Fig 3), CMP

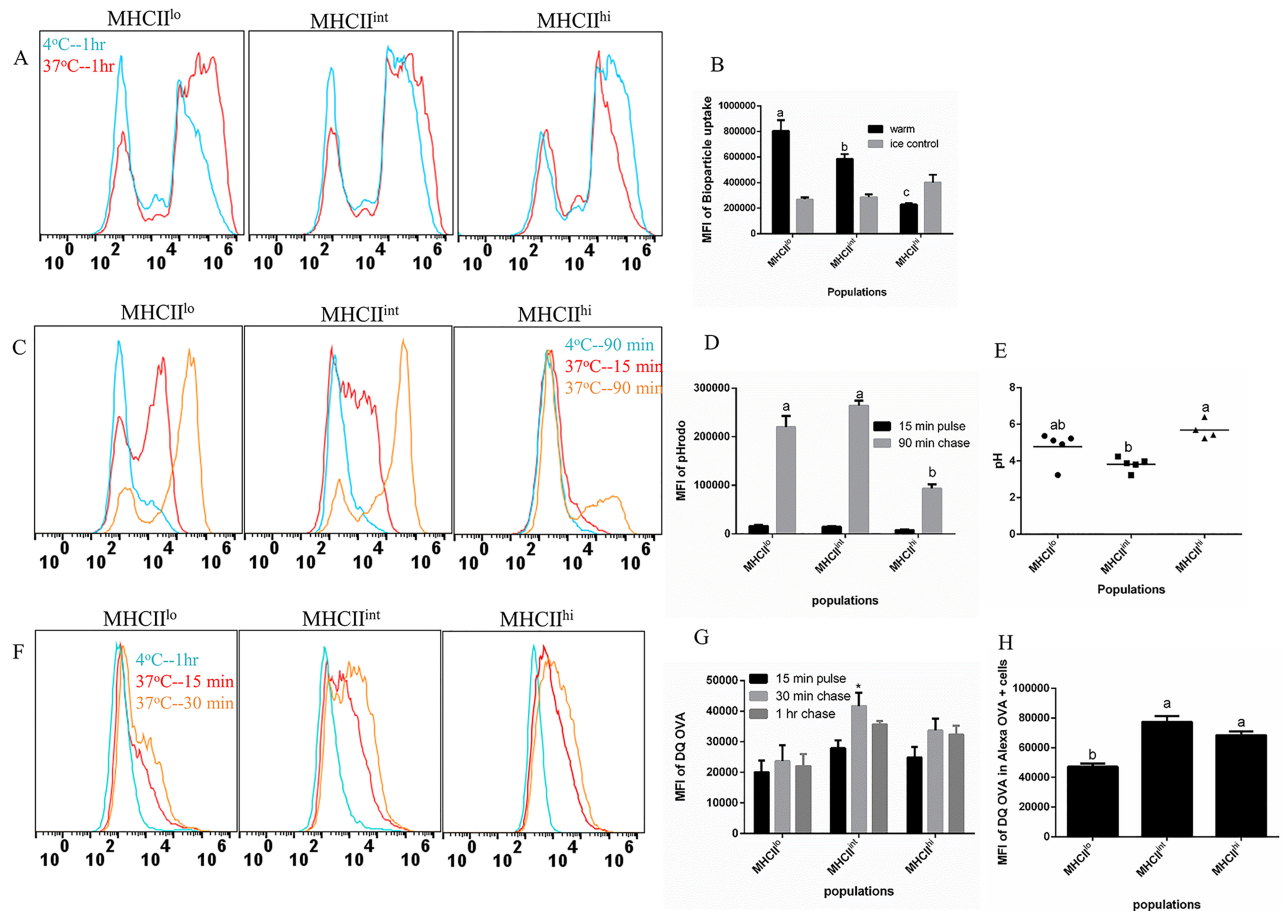


**Fig 6. The MHCII<sup>lo</sup> and MHCII<sup>int</sup> cell populations are similar in uptake capacity and phagosomal acidification when compared with MHCII<sup>hi</sup> cells.** Cells were sorted into three populations on day 5 of culture: MHCII<sup>lo</sup>, MHCII<sup>int</sup> and MHCII<sup>hi</sup> after first gating on CD11c<sup>+</sup>, and CD11b<sup>+</sup> cells. (A) Sorted cells were fed *S. aureus* BioParticle-Alexa flour 594 conjugate for 1 h. Representative histograms of BioParticle uptake at 4°C (blue) or 37°C (red). (B) Compiled MFI of BioParticle uptake from three experiments. (C) Representative histograms of cells pulsed with pHrodo *E. coli* BioParticles at 15 min (red) and chased for 90 min (brown) or at 4°C for 90 min (blue). (D) The compiled MFI of pHrodo *E. coli* BioParticle at 15 min and 90 min. (E) Calculated phagosomal pH of each cell population based on standard curves. (F) Representative histograms of cells pulsed with 10 µg/mL DQ-OVA for 15 min (red) and chased for 30 min (brown) or at 4°C for 1 hr (blue). (G) Compiled MFI of DQ-OVA at 15 min and degradation at 30 min and 1hr. (H) The compiled MFI of DQ-OVA degradation within OVA-Alexa positive cells measured at 1 hr post incubation. Statistical analysis was performed using SAS, one-way ANOVA Tukey's multiple comparison test. Letters over bars indicate statistically significant differences in means (p<0.05).

<https://doi.org/10.1371/journal.pone.0196591.g006>

isolated *ex vivo* had the highest phagosomal pH (pH ~7.14), with GMP having an average pH of 6.42, while monocytes had a slightly more acidic pH (pH ~5.92) (Fig 7C, 7D and 7E). Lastly, we observed that CMP had the least proteolytic capacity when compared with GMP (Fig 7F). Thus, we conclude that our *in vitro* cultured cells: CMP, GMP and monocytes closely resemble their *ex vivo* counterparts.

## Discussion

Most studies of DC function such as endocytosis, proteolysis, and antigen processing and presenting function have focused on fully differentiated DC. As a result, less is known about when these cellular mechanisms develop or how they change as myeloid cells progress from progenitor cells to more differentiated cell types. In this study, we have now determined that as the cells develop, they undergo significant changes in phenotypic and functional characteristics

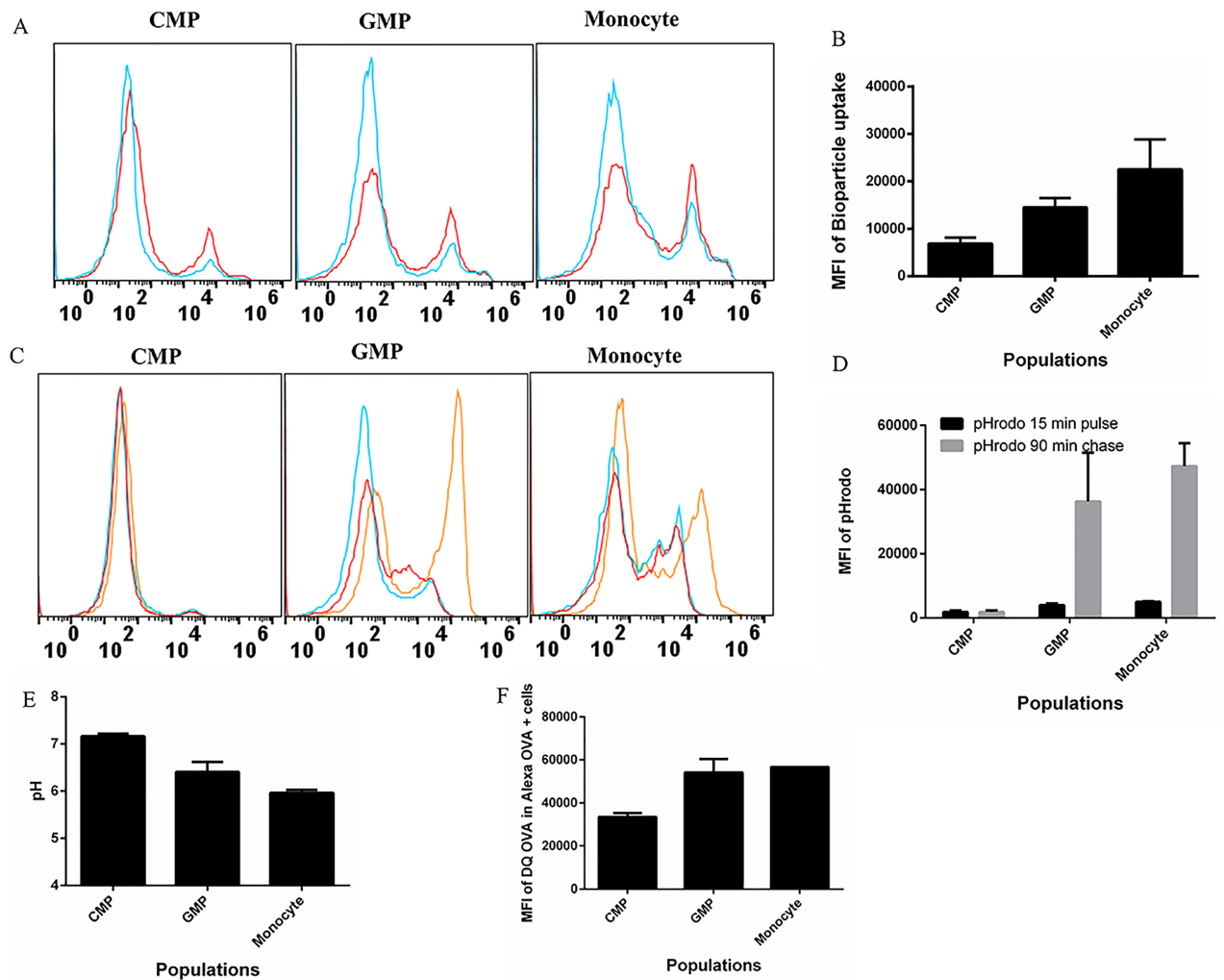


**Fig 7. CMP, GMP and monocyte derived *ex-vivo* are similar in functionality to *in vitro* GM-CSF derived counterpart.** Freshly harvested *ex-vivo* bone marrow cells were sorted into 3 populations as previously described. (A) Sorted cells were fed *E. coli* BioParticle-Alexa flour 594 conjugate for 1 h. Representative histograms of BioParticle uptake at 4°C (blue) or 37°C (red). (B) Compiled MFI of BioParticle uptake from three experiments. (C) Representative histograms of cells pulsed with pHrodo *E. coli* BioParticles at 15 min (red) and chased for 90 min (brown) or at 4°C for 90 min (blue). (D) The compiled MFI of pHrodo *E. coli* BioParticle at 15 min and 90 min. (E) Calculated phagosomal pH of each cell population based on standard curves. (F) The compiled MFI of DQ-OVA degradation within OVA-Alexa positive cells measured at 1 hr post incubation.

<https://doi.org/10.1371/journal.pone.0196591.g007>

including: expression of uptake receptors, endocytic capacity, phagosomal pH, proteolytic activity, and antigen processing and presenting capacity.

CMPs, the earliest cell type examined demonstrated little endocytic or phagocytic activity, low proteolytic potential, and the highest phagosomal pH of all of the populations, at near neutral. CMPs are progenitor cells that have the ability to give rise to all the myeloid cells [47]. As such, CMPs have not yet developed all the necessary cellular machinery that could either enhance their antigen uptake capacity or degradative potential. In addition, CMPs had little ability to induce T cell proliferation or activation. CMPs showed the lowest response in all of the functional analyses in this study. However, this does not indicate that these cells are functionally incompetent. As such, a recent study illustrated the immune suppressive activity of CMP and GMP in the context of tumors as evidence in the ability of these cells to inhibit T cell



proliferation [48]. Taken together, our study shows that CMPs are not potent at inducing T cell activation, but does not rule out a role for these cells in immune regulation.

GMP, the second stage along the GM-CSF-driven developmental spectrum, demonstrated high phagocytic capacity, moderate proteolysis and slightly more acidic phagosomal pH. Also, GMP demonstrated only slight antigen presentation function, evidenced in their ability to present OVA peptide to CD8<sup>+</sup> T cells (Fig 5D). This observation might be attributed to the fact that innate immune cells constitutively express MHC class I molecules, potentially accounting for the ability of GMP to induce CD8<sup>+</sup> T cell proliferation. However, GMPs were only able to induce CD8<sup>+</sup> T cell proliferation without activation, as evidenced in low expression of CD25. In addition, GMP had lower expression of MHC class II, which could explain the inability of these cells to induce CD4<sup>+</sup> T cell proliferation.

Monocytes had the highest phagocytic capability, and high expression of the uptake receptors when compared with CMP and GMP. The high uptake potential observed in monocytes was expected because these cells are known to be highly phagocytic, and they are endowed with a large repertoire of uptake receptors [49]. In addition, monocytes demonstrated high proteolytic capacity and low phagosomal pH, two functional properties that also support the antimicrobial activities of this cell type [50]. There have been conflicting results about the role of monocytes in antigen processing and presentation. For instance, a recent study demonstrated that Ly6C<sup>+</sup> monocytes can cross-present cell-associated antigen to CD8<sup>+</sup> T cells in a manner similar to DC [51], while another showed that monocytes are poor at presenting antigen [10]. In this study, we observed that within this population, antigen processing and presentation functions started to develop as evidenced in their ability to induce minimal CD4<sup>+</sup> T cell proliferation when given OVA protein. Notably, monocytes were poor at presenting OVA peptide to naïve CD4<sup>+</sup> T cells when compared with moMac/moDP and moDC (Fig 5A). Perhaps the peptide was less stable in this population. However, we observed that monocytes could cross present OVA protein to CD8<sup>+</sup> T cells and induce T cell proliferation.

moMac/moDP includes cell types that phenotypically resemble macrophages as well as precursor cells, moDP, that can further differentiate to moDC [33]. Thus, some of the functional characteristics of the moMac/moDP cell population closely resemble moDC. First, we observed that moMac/moDP had high expression of uptake receptors and moderate uptake of BioParticles and dextran when compared with monocytes. In addition, the kinetics of proteolytic activities showed that moMac/moDP had high degradative capacity and the lowest phagosomal pH when compared with other cell types. Macrophages are known to have antimicrobial properties and are highly degradative, in line with their function in clearance of invading microbes [52].

While this is the first study examining the function of moDP, the functional characteristics of moMac have been more extensively studied. The moMac can acquire different functional attributes depending on the environmental cues, activation status, and inflammatory signals [53–55]. In addition, moMac can change their phenotype from a proinflammatory mediator to anti-inflammatory mediator and vice-versa, demonstrating their functional plasticity [56, 57]. To further determine the functional differences between the moMac and moDP, the mixed cell population was separated into three distinct populations based on the expression of MHCII. When we compared uptake capacity in MHCII<sup>low</sup> and MHCII<sup>int</sup> populations, corresponding to moMac and moDP respectively, we observed that the moMac cell population demonstrated higher uptake capacity than moDP, and moDC (MHCII<sup>hi</sup> population) (Fig 6A). Although different moMac populations have been shown to differ to some extent in phagocytic capacity [53, 58] owing to the distinct array of uptake receptors they express [59], moMac generally have a higher uptake capacity when compared with DC [53]. This observation was consistent with our results.

Moreover, the phagosomal pH of different macrophage subtypes may also be distinct. For example, pro-inflammatory macrophages maintaining a pH close to neutral while the anti-inflammatory macrophages rapidly acidify their phagosomes [29]. When we examined the phagosome acidification in moMac and moDP, we observed that both cell populations had lower phagosomal pH when compared with moDC (MHCII<sup>hi</sup> population) (Fig 6). The highly efficient phagosomal acidification observed in moMac/moDP could make this cell better suited at controlling microbes, a function that will need to be further examined. Finally, moDP had a slightly higher proteolytic activity when compared with moMac.

Intriguingly, we found that antigen processing and presenting functions develop before GM-CSF driven myeloid cells became fully differentiated moDC. moMac/moDP had a strong ability to induce CD4<sup>+</sup> T cell proliferation and activation at a rate that is comparable with moDC. The ability of moMac/moDP to stimulate CD4<sup>+</sup> T cell activation was greater than that observed in GM-Macs, a cell type highlighted by Helft et.al (similar to moMac in our study) [31]. Our data demonstrated that moMac/moDP is a unique mixture of cell types including those with similarity to GM-Macs, but also potent at priming naïve CD4<sup>+</sup> T cells in a manner similar to moDC. This potent T cell activation capacity is likely mediated by the moDP population present in this complex population.

moDC functions are well characterized in the literature. It is well established that as DCs mature, they down-regulate their uptake mechanisms in favor of presenting the processed antigen via MHC on the cell surface [26, 41]. The observed decrease in uptake of BioParticles by moDC when compared with moDP (Fig 2C) could be a result of moDC being more differentiated and having less phagocytic activity. However, the uptake of dextran in both moMac/moDP and moDC reflects their ability to continuously take in bulk extracellular fluid, likely by macropinocytosis. In addition, moDC demonstrated a similar proteolytic activity and slightly higher phagosomal pH than moMac/moDP. These observed differences between moMac/moDP and moDC might be because moDC are more differentiated. In fact, several studies have indicated that DC have low degradative potential and high phagosomal pH, allowing for preservation of antigen for immune recognition [52, 60, 61]. Interestingly, phagosomal pH is known to decrease at least initially upon DC maturation, attributed to full assembly of vATPase on the mature DC phagosomal membranes [26]. Future studies in this arena should thus include an examination of vATPase assembly and activity in developing cells. Among all cell types examined in this study, we found that moDC were most potent at inducing both CD4<sup>+</sup> and CD8<sup>+</sup> T cell proliferation and activation, reaffirming their status as professional antigen presenting cells.

In summary, we have been able to systematically show the function of distinct myeloid cell populations during GM-CSF driven differentiation and how these functions change as the cells progress through their development. Importantly, we have been able to demonstrate in this study that antigen processing and presenting capability is a function that is acquired prior to the cells becoming moDC. This insight is essential because it could enhance the utilization of most qualified cells to function as antigen presenting cells in the design of vaccines.

## Supporting information

**S1 Fig. The expression of MHC class I and MHC class II molecules during GM-CSF driven differentiation.** Sorted cells were stained with antibodies to Ly6C, CD115, and CD11c. (A) MFI of MHC class I and (B) MHC class II expression in the five cell populations. (TIF)

**S2 Fig. Histogram depiction of T cell activation from Fig 5.** (A) The histogram depicts CFSE fluorescence dilution in CD4<sup>+</sup> OT-II T cells stimulated with 1  $\mu$ M of OVA<sub>323-339</sub> (top) or



100 µg/mL of OVA protein (bottom). (B) and (C) Compiled data of absolute number of OT-II T cells in the presence of OVA peptide (1 µM) or OVA protein (100 µg/mL), respectively. (D) The histogram of CFSE fluorescence dilution in CD8<sup>+</sup> OT-I T cells stimulated with 10 nM of OVA<sub>257-264</sub> (top) or 300 µg/mL of OVA protein (bottom). (E) and (F) The absolute number of OT-I T cells in the presence of OVA peptide (10 nM) or OVA protein (300 µg/mL), respectively. (TIF)

## Acknowledgments

We are grateful to Alison Church Bird and the flow cytometry core facility at Auburn University for cell sorting. This work was supported by grant R15 AI107773 from the National Institutes of Health/NIAID to EHS.

## Author Contributions

**Conceptualization:** Elizabeth Hiltbold Schwartz.

**Data curation:** Adesola C. Olatunde.

**Formal analysis:** Adesola C. Olatunde, Elizabeth Hiltbold Schwartz.

**Funding acquisition:** Elizabeth Hiltbold Schwartz.

**Investigation:** Adesola C. Olatunde, Laura P. Abell, Ashley E. Landuyt.

**Methodology:** Adesola C. Olatunde, Laura P. Abell, Ashley E. Landuyt.

**Project administration:** Elizabeth Hiltbold Schwartz.

**Supervision:** Elizabeth Hiltbold Schwartz.

**Validation:** Ashley E. Landuyt.

**Visualization:** Adesola C. Olatunde.

**Writing – original draft:** Adesola C. Olatunde.

**Writing – review & editing:** Elizabeth Hiltbold Schwartz.

## References

1. Roche PA, Furuta K. The ins and outs of MHC class II-mediated antigen processing and presentation. *Nature Reviews Immunology*. 2015; 15(4):203–16. <https://doi.org/10.1038/nri3818> PMID: 25720354
2. Dudziak D, Kamphorst AO, Heidkamp GF, Buchholz VR, Trumpheller C, Yamazaki S, et al. Differential antigen processing by dendritic cell subsets in vivo. *Science*. 2007; 315(5808):107–11. <https://doi.org/10.1126/science.1136080> PMID: 17204652
3. León B, López-Bravo M, Ardavin C. Monocyte-derived dendritic cells formed at the infection site control the induction of protective T helper 1 responses against *Leishmania*. *Immunity*. 2007; 26(4):519–31. <https://doi.org/10.1016/j.immuni.2007.01.017> PMID: 17412618
4. Merad M, Sathe P, Helft J, Miller J, Mortha A. The dendritic cell lineage: ontogeny and function of dendritic cells and their subsets in the steady state and the inflamed setting. *Annual review of immunology*. 2013; 31.
5. Mildner A, Jung S. Development and Function of Dendritic Cell Subsets. *Immunity*. 2014; 40(5):642–56. <https://doi.org/10.1016/j.immuni.2014.04.016> PMID: 24837101
6. Vremec D, Pooley J, Hochrein H, Wu L, Shortman K. CD4 and CD8 expression by dendritic cell subtypes in mouse thymus and spleen. *The Journal of Immunology*. 2000; 164(6):2978–86. PMID: 10706685

7. Varol C, Vallon-Eberhard A, Elinav E, Aychek T, Shapira Y, Luche H, et al. Intestinal lamina propria dendritic cell subsets have different origin and functions. *Immunity*. 2009; 31(3):502–12. <https://doi.org/10.1016/j.immuni.2009.06.025> PMID: 19733097
8. Bogunovic M, Ginhoux F, Helft J, Shang L, Hashimoto D, Greter M, et al. Origin of the lamina propria dendritic cell network. *Immunity*. 2009; 31(3):513–25. <https://doi.org/10.1016/j.immuni.2009.08.010> PMID: 19733489
9. Randolph GJ, Ochando J, Partida-Sánchez S. Migration of dendritic cell subsets and their precursors. *Annu Rev Immunol*. 2008; 26:293–316. <https://doi.org/10.1146/annurev.immunol.26.021607.090254> PMID: 18045026
10. Kamphorst AO, Guermontprez P, Dudziak D, Nussenzweig MC. Route of antigen uptake differentially impacts presentation by dendritic cells and activated monocytes. *The Journal of Immunology*. 2010; 185(6):3426–35. <https://doi.org/10.4049/jimmunol.1001205> PMID: 20729332
11. Waskow C, Liu K, Darrasse-Jèze G, Guermontprez P, Ginhoux F, Merad M, et al. FMS-like tyrosine kinase 3 is required for dendritic cell development in peripheral lymphoid tissues. *Nature immunology*. 2008; 9(6):676.
12. Onai N, Obata-Onai A, Schmid MA, Ohteki T, Jarrossay D, Manz MG. Identification of clonogenic common Flt3+ M-CSFR+ plasmacytoid and conventional dendritic cell progenitors in mouse bone marrow. *Nature immunology*. 2007; 8(11):1207. <https://doi.org/10.1038/ni1518> PMID: 17922016
13. Naik SH, Sathe P, Park H-Y, Metcalf D, Proietto AI, Dakic A, et al. Development of plasmacytoid and conventional dendritic cell subtypes from single precursor cells derived in vitro and in vivo. *Nature immunology*. 2007; 8(11):1217–26. <https://doi.org/10.1038/ni1522> PMID: 17922015
14. D'Amico A, Wu L. The early progenitors of mouse dendritic cells and plasmacytoid predendritic cells are within the bone marrow hemopoietic precursors expressing Flt3. *Journal of Experimental Medicine*. 2003; 198(2):293–303. <https://doi.org/10.1084/jem.20030107> PMID: 12874262
15. Karsunky H, Merad M, Cozzio A, Weissman IL, Manz MG. Flt3 ligand regulates dendritic cell development from Flt3+ lymphoid and myeloid-committed progenitors to Flt3+ dendritic cells in vivo. *The Journal of experimental medicine*. 2003; 198(2):305–13. <https://doi.org/10.1084/jem.20030323> PMID: 12874263
16. Naik SH, Proietto AI, Wilson NS, Dakic A, Schnorrer P, Fuchsberger M, et al. Cutting edge: generation of splenic CD8+ and CD8- dendritic cell equivalents in Fms-like tyrosine kinase 3 ligand bone marrow cultures. *The Journal of Immunology*. 2005; 174(11):6592–7. PMID: 15905497
17. Naik SH, Metcalf D, van Nieuwenhuijze A, Wicks I, Wu L, O'Keeffe M, et al. Intrasplenic steady-state dendritic cell precursors that are distinct from monocytes. *Nature immunology*. 2006; 7(6):663–71. <https://doi.org/10.1038/ni1340> PMID: 16680143
18. Shortman K, Naik SH. Steady-state and inflammatory dendritic-cell development. *Nature Reviews Immunology*. 2007; 7(1):19–30. <https://doi.org/10.1038/nri1996> PMID: 17170756
19. van de Laar L, Coffey PJ, Woltman AM. Regulation of dendritic cell development by GM-CSF: molecular control and implications for immune homeostasis and therapy. *Blood*. 2012; 119(15):3383–93. <https://doi.org/10.1182/blood-2011-11-370130> PMID: 22323450
20. Xu Y, Zhan Y, Lew AM, Naik SH, Kershaw MH. Differential development of murine dendritic cells by GM-CSF versus Flt3 ligand has implications for inflammation and trafficking. *The Journal of Immunology*. 2007; 179(11):7577–84. PMID: 18025203
21. Louis C, Cook AD, Lacey D, Fleetwood AJ, Vlahos R, Anderson GP, et al. Specific contributions of CSF-1 and GM-CSF to the dynamics of the mononuclear phagocyte system. *The Journal of Immunology*. 2015; 195(1):134–44. <https://doi.org/10.4049/jimmunol.1500369> PMID: 26019271
22. Van Voorhis WC, Hair LS, Steinman RM, Kaplan G. Human dendritic cells. Enrichment and characterization from peripheral blood. *Journal of Experimental Medicine*. 1982; 155(4):1172–87. PMID: 6460832
23. Inaba K, Inaba M, Romani N, Aya H, Deguchi M, Ikehara S, et al. Generation of large numbers of dendritic cells from mouse bone marrow cultures supplemented with granulocyte/macrophage colony-stimulating factor. *Journal of Experimental Medicine*. 1992; 176:1693-. PMID: 1460426
24. Caux C, Vanbervliet B, Massacrier C, Dezutter-Dambuyant C, De Saint-Vis B, Jacquet C, et al. CD34<sup>+</sup> hematopoietic progenitors from human cord blood differentiate along two independent dendritic cell pathways in response to GM-CSF+ TNF. *Journal of Experimental Medicine*. 1996; 184:695–706. PMID: 8760823
25. Sallusto F, Lanzavecchia A. Efficient presentation of soluble antigen by cultured human dendritic cells is maintained by granulocyte/macrophage colony-stimulating factor plus interleukin 4 and downregulated by tumor necrosis factor. *Journal of Experimental Medicine*. 1994; 179(4):1109–18. PMID: 8145033

26. Mellman I, Steinman RM. Dendritic Cells—Specialized and Regulated Antigen Processing Machines. *Cell*. 2001; 106(3):255–8. PMID: [11509172](https://pubmed.ncbi.nlm.nih.gov/11509172/)
27. Savina A, Amigorena S. Phagocytosis and antigen presentation in dendritic cells. *Immunological reviews*. 2007; 219(1):143–56.
28. Savina A, Jancic C, Hugues S, Guermonprez P, Vargas P, Moura IC, et al. NOX2 controls phagosomal pH to regulate antigen processing during crosspresentation by dendritic cells. *Cell*. 2006; 126(1):205–18. <https://doi.org/10.1016/j.cell.2006.05.035> PMID: [16839887](https://pubmed.ncbi.nlm.nih.gov/16839887/)
29. Canton J, Khezri R, Glogauer M, Grinstein S. Contrasting phagosome pH regulation and maturation in human M1 and M2 macrophages. *Molecular biology of the cell*. 2014; 25(21):3330–41. <https://doi.org/10.1091/mbc.E14-05-0967> PMID: [25165138](https://pubmed.ncbi.nlm.nih.gov/25165138/)
30. Alloatti A, Kotsias F, Pauwels A-M, Carpier J-M, Jouve M, Timmerman E, et al. Toll-like receptor 4 engagement on dendritic cells restrains phago-lysosome fusion and promotes cross-presentation of antigens. *Immunity*. 2015; 43(6):1087–100. <https://doi.org/10.1016/j.immuni.2015.11.006> PMID: [26682983](https://pubmed.ncbi.nlm.nih.gov/26682983/)
31. Helft J, Böttcher J, Chakravarty P, Zelenay S, Huotari J, Schraml BU, et al. GM-CSF mouse bone marrow cultures comprise a heterogeneous population of CD11c+ MHCII+ macrophages and dendritic cells. *Immunity*. 2015; 42(6):1197–211. <https://doi.org/10.1016/j.immuni.2015.05.018> PMID: [26084029](https://pubmed.ncbi.nlm.nih.gov/26084029/)
32. Na YR, Jung D, Gu GJ, Seok SH. GM-CSF Grown Bone Marrow Derived Cells Are Composed of Phenotypically Different Dendritic Cells and Macrophages. *Molecules and Cells*. 2016; 39(10):734. <https://doi.org/10.14348/molcells.2016.0160> PMID: [27788572](https://pubmed.ncbi.nlm.nih.gov/27788572/)
33. Rogers P, Driessnack M, Hiltbold SE. Analysis of the developmental stages, kinetics, and phenotypes exhibited by myeloid cells driven by GM-CSF in vitro. *PLoS one*. 2017; 12(7):e0181985. <https://doi.org/10.1371/journal.pone.0181985> PMID: [28750033](https://pubmed.ncbi.nlm.nih.gov/28750033/)
34. Westcott MM, Henry CJ, Amis JE, Hiltbold EM. Dendritic cells inhibit the progression of *Listeria monocytogenes* intracellular infection by retaining bacteria in major histocompatibility complex class II-rich phagosomes and by limiting cytosolic growth. *Infection and immunity*. 2010; 78(7):2956–65. <https://doi.org/10.1128/IAI.01027-09> PMID: [20404078](https://pubmed.ncbi.nlm.nih.gov/20404078/)
35. Areschoug T, Gordon S. Scavenger receptors: role in innate immunity and microbial pathogenesis. *Cellular microbiology*. 2009; 11(8):1160–9. <https://doi.org/10.1111/j.1462-5822.2009.01326.x> PMID: [19388903](https://pubmed.ncbi.nlm.nih.gov/19388903/)
36. Sharif O, Matt U, Saluzzo S, Lakovits K, Haslinger I, Furtner T, et al. The scavenger receptor CD36 downmodulates the early inflammatory response while enhancing bacterial phagocytosis during pneumococcal pneumonia. *The Journal of Immunology*. 2013; 190(11):5640–8. <https://doi.org/10.4049/jimmunol.1202270> PMID: [23610144](https://pubmed.ncbi.nlm.nih.gov/23610144/)
37. Józefowski S, Yang Z, Marcinkiewicz J, Kobzik L. Scavenger receptors and  $\beta$ -glucan receptors participate in the recognition of yeasts by murine macrophages. *Inflammation Research*. 2012; 61(2):113–26. <https://doi.org/10.1007/s00011-011-0395-5> PMID: [22116297](https://pubmed.ncbi.nlm.nih.gov/22116297/)
38. Lefèvre L, Lugo-Villarino G, Meunier E, Valentin A, Olagnier D, Authier H, et al. The C-type lectin receptors dectin-1, MR, and SIGNR3 contribute both positively and negatively to the macrophage response to *Leishmania infantum*. *Immunity*. 2013; 38(5):1038–49. <https://doi.org/10.1016/j.immuni.2013.04.010> PMID: [23684988](https://pubmed.ncbi.nlm.nih.gov/23684988/)
39. Amiel E, Nicholson-Dykstra S, Walters JJ, Higgs H, Berwin B. Scavenger receptor-A functions in phagocytosis of *E. coli* by bone marrow dendritic cells. *Experimental cell research*. 2007; 313(7):1438–48. <https://doi.org/10.1016/j.yexcr.2007.02.011> PMID: [17362929](https://pubmed.ncbi.nlm.nih.gov/17362929/)
40. Platt CD, Ma JK, Chalouni C, Ebersold M, Bou-Reslan H, Carano RA, et al. Mature dendritic cells use endocytic receptors to capture and present antigens. *Proceedings of the National Academy of Sciences*. 2010; 107(9):4287–92.
41. Garrett WS, Chen L-M, Kroschewski R, Ebersold M, Turley S, Trombetta S, et al. Developmental control of endocytosis in dendritic cells by Cdc42. *Cell*. 2000; 102(3):325–34. PMID: [10975523](https://pubmed.ncbi.nlm.nih.gov/10975523/)
42. Sallusto F, Cella M, Danieli C, Lanzavecchia A. Dendritic cells use macropinocytosis and the mannose receptor to concentrate macromolecules in the major histocompatibility complex class II compartment: downregulation by cytokines and bacterial products. *The Journal of experimental medicine*. 1995; 182(2):389–400. PMID: [7629501](https://pubmed.ncbi.nlm.nih.gov/7629501/)
43. West MA, Wallin RP, Matthews SP, Svensson HG, Zaru R, Ljunggren H-G, et al. Enhanced dendritic cell antigen capture via toll-like receptor-induced actin remodeling. *Science*. 2004; 305(5687):1153–7. <https://doi.org/10.1126/science.1099153> PMID: [15326355](https://pubmed.ncbi.nlm.nih.gov/15326355/)
44. Blander JM, Medzhitov R. On regulation of phagosome maturation and antigen presentation. *Nature immunology*. 2006; 7(10):1029–35. <https://doi.org/10.1038/ni1006-1029> PMID: [16985500](https://pubmed.ncbi.nlm.nih.gov/16985500/)

45. Ip WE, Sokolovska A, Charriere GM, Boyer L, Dejardin S, Cappillino MP, et al. Phagocytosis and phagosome acidification are required for pathogen processing and MyD88-dependent responses to *Staphylococcus aureus*. *The Journal of Immunology*. 2010; 184(12):7071–81. <https://doi.org/10.4049/jimmunol.1000110> PMID: 20483752
46. Westcott MM, Henry CJ, Cook AS, Grant KW, Hiltbold EM. Differential susceptibility of bone marrow-derived dendritic cells and macrophages to productive infection with *Listeria monocytogenes*. *Cellular microbiology*. 2007; 9(6):1397–411. <https://doi.org/10.1111/j.1462-5822.2006.00880.x> PMID: 17250592
47. Akashi K, Traver D, Miyamoto T, Weissman IL. A clonogenic common myeloid progenitor that gives rise to all myeloid lineages. *Nature*. 2000; 404(6774):193–7. <https://doi.org/10.1038/35004599> PMID: 10724173
48. Pu S, Qin B, He H, Zhan J, Wu Q, Zhang X, et al. Identification of early myeloid progenitors as immunosuppressive cells. *Scientific reports*. 2016; 6.
49. Dale DC, Boxer L, Liles WC. The phagocytes: neutrophils and monocytes. *Blood*. 2008; 112(4):935–45. <https://doi.org/10.1182/blood-2007-12-077917> PMID: 18684880
50. Serbina NV, Shi C, Pamer EG. Monocyte-mediated immune defense against murine *Listeria monocytogenes* infection. *Advances in immunology*. 2012; 113:119. <https://doi.org/10.1016/B978-0-12-394590-7.00003-8> PMID: 22244581
51. Larson S, Atif S, Gibbings S, Thomas S, Prabagar M, Danhorn T, et al. Ly6C+ monocyte efferocytosis and cross-presentation of cell-associated antigens. *Cell death and differentiation*. 2016; 23(6):997. <https://doi.org/10.1038/cdd.2016.24> PMID: 26990659
52. Savina A, Peres A, Cebrian I, Carmo N, Moita C, Hacohen N, et al. The small GTPase Rac2 controls phagosomal alkalinization and antigen crosspresentation selectively in CD8+ dendritic cells. *Immunity*. 2009; 30(4):544–55. <https://doi.org/10.1016/j.immuni.2009.01.013> PMID: 19328020
53. Xu W, Roos A, Schlagwein N, Woltman AM, Daha MR, van Kooten C. IL-10-producing macrophages preferentially clear early apoptotic cells. *Blood*. 2006; 107(12):4930–7. <https://doi.org/10.1182/blood-2005-10-4144> PMID: 16497970
54. Rey-Giraud F, Hafner M, Ries CH. In vitro generation of monocyte-derived macrophages under serum-free conditions improves their tumor promoting functions. *PloS one*. 2012; 7(8):e42656. <https://doi.org/10.1371/journal.pone.0042656> PMID: 22880072
55. Savage ND, de Boer T, Walburg KV, Joosten SA, van Meijgaarden K, Geluk A, et al. Human anti-inflammatory macrophages induce Foxp3+ GITR+ CD25+ regulatory T cells, which suppress via membrane-bound TGFβ-1. *The Journal of Immunology*. 2008; 181(3):2220–6. PMID: 18641362
56. Wattananit S, Tornero D, Graubardt N, Memanishvili T, Monni E, Tatarishvili J, et al. Monocyte-derived macrophages contribute to spontaneous long-term functional recovery after stroke in mice. *Journal of Neuroscience*. 2016; 36(15):4182–95. <https://doi.org/10.1523/JNEUROSCI.4317-15.2016> PMID: 27076418
57. Heusinkveld M, van Steenwijk PJdV, Goedemans R, Ramwadhoebe TH, Gorter A, Welters MJ, et al. M2 macrophages induced by prostaglandin E2 and IL-6 from cervical carcinoma are switched to activated M1 macrophages by CD4+ Th1 cells. *The Journal of Immunology*. 2011; 187(3):1157–65. <https://doi.org/10.4049/jimmunol.1100889> PMID: 21709158
58. Eligini S, Crisci M, Bono E, Songia P, Tremoli E, Colombo GI, et al. Human monocyte-derived macrophages spontaneously differentiated in vitro show distinct phenotypes. *Journal of cellular physiology*. 2013; 228(7):1464–72. <https://doi.org/10.1002/jcp.24301> PMID: 23255209
59. Levin R, Grinstein S, Canton J. The life cycle of phagosomes: formation, maturation, and resolution. *Immunological reviews*. 2016; 273(1):156–79. <https://doi.org/10.1111/imr.12439> PMID: 27558334
60. Delamarre L, Pack M, Chang H, Mellman I, Trombetta ES. Differential lysosomal proteolysis in antigen-presenting cells determines antigen fate. *Science*. 2005; 307(5715):1630–4. <https://doi.org/10.1126/science.1108003> PMID: 15761154
61. Trombetta ES, Ebersold M, Garrett W, Pypaert M, Mellman I. Activation of lysosomal function during dendritic cell maturation. *Science*. 2003; 299(5611):1400–3. <https://doi.org/10.1126/science.1080106> PMID: 12610307